CHINESE OPTICS LETTERS

Vol. 19, No. 4 | April 2021

Highly sensitive torsion sensor based on triangular-prism-shaped long-period fiber gratings

Senyu Wang (王森宇)[1], Yiwei Ma (马一巍)[1], Xiaoyang Li (李晓飏)[1], Yang Yi (易 杨)[1], Cuiting Sun (孙翠婷)[1], Jingyu Lin (林静雨)[1], Chengguo Tong (佟成国)[2], Yuxiang Li (李玉祥)[1*], Tao Geng (耿 涛)[1**], Weimin Sun (孙伟民)[1], and Libo Yuan (苑立波)[2]

[1] College of Science, Harbin Engineering University, Harbin 150001, China

[2] Photonics Research Center, Guilin University of Electronics Technology, Guilin 541004, China

*Corresponding author: liyuxiang11@hrbeu.edu.cn

**Corresponding author: gengtao_hit_oe@126.com

Received May 19, 2020 | Accepted October 19, 2020 | Posted Online January 13, 2021

We propose and investigate a compact optical fiber sensor that aims to measure the torsion in both amount and direction with high sensitivity. This sensor is configured by a triangular-prism-shaped long-period fiber grating, which is fabricated by the high frequency CO_2 laser polished method. The unique design of the triangular-shaped structure breaks the rotational symmetry of the optical fiber and provides high sensitivity for torsion measurement. In preliminary experiments, the torsion response of the sensor achieves a good stability and linearity. The torsion sensitivity is 0.54 nm/(rad/m), which renders the proposed structure a highly sensitive torsion sensor.

Keywords: long-period fiber grating; torsion sensor; CO_2 laser etched method.

DOI: 10.3788/COL202119.041202

1. Introduction

Torsion measurement plays an important role in many fields such as structural health monitoring, anthropomorphic robots, aerospace engineering, and the automotive industry[1,2]. Recently, long-period fiber gratings (LPFGs) have been widely used in torsion sensors due to their advantages, such as easy fabrication, small volume, light weight, high sensitivity, and anti-electromagnetic noise[3,4]. Hence, various torsion sensors based on LPFG have been reported. The fabrication methods of LPFG sensors include acid etching[5], UV laser radiating[6], and CO_2 laser writing[7]. However, LPFGs fabricated by the first two methods are unable to distinguish the torsion direction. Such an issue brings difficulty for practical applications, which requires the information about the torsion direction. The fabrication method based on CO_2 laser writing gives LPFGs the ability to determine the torsion direction. The basic principle follows that the elliptic birefringence is excited in the structure. The sensitivity of torsion sensors of such a kind is around 0.03 nm/(rad/m)[8], which requires a higher precision of demodulation equipment to monitor the changes of resonant wavelength. To further improve the torsion sensitivity of LPFGs, certain structures are proposed and demonstrated in recent studies, including the LPFG that is based on periodical screw-type distortions[9], the helical LPFG (HLPFG)[10], and the segmented LPFG[11]. However, these structures require devices with high precision, which increases the cost. In addition, the fabricating process of these structures is complex. Hence, optical torsion sensors with the advantages of high sensitivity and simple fabrication process are expected.

In this work, we propose and fabricate a miniature triangular-prism-shaped LPFG (TPS-LPFG) torsion sensor by using the CO_2 laser polished method. This method has the ability to change the physical shape of fiber cladding flexibly. In order to improve the torsion sensitivity of the sensor effectively, the triangular-shaped structure is designed. This structure provides the high sensitivity of torsion, which results from the broken rotational symmetry of the fiber. In torsion measurement, the sensitivity of the TPS-LPFG is 0.54 nm/(rad/m), which is about 18 times higher than that of the conventional LPFG[8]. Moreover, this structure has the advantages of compact size, low budget, and easy fabrication. Therefore, the proposed sensor based on TPS-LPFG has good potential in torsion measurement of small structures.

2. Fabrication and Principle

In order to fabricate the proposed structure, the LPFG inscribing platform has been set up, as shown in Fig. 1. A high frequency CO_2 laser with a maximum output power of 10 W is used to polish the fiber. It is controlled by a host computer. An optical

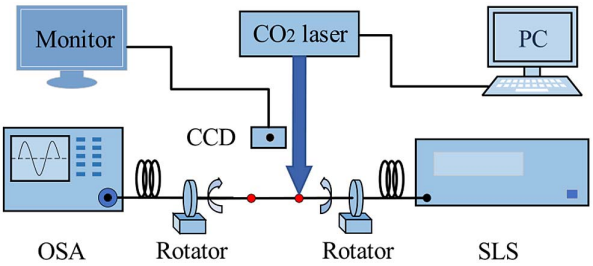

Fig. 1. Diagram of the TPS-LPFG fabricating system.

spectrum analyzer (OSA) and a super-continuum light source (SLS) are used to detect the light signal and provide the input light, respectively. The side view of the structure is captured by the charge-coupled device (CCD). In the preparation process, a single mode fiber (SMF) is selected for fabrication of the TPS-LPFG through the CO_2 laser polished method. First, the SMF is fixed on the middle of two rotating disks. To keep the interested part of SMF in a straight line, a constant axial force is applied by a 5 g weight, which is attached to the fiber. The distance between two rotating disks is 20 cm. Then, a CO_2 laser is used to polish the fiber. The reduction of diameter in the fiber cladding is performed by the continuous laser exposure with the power of 1.8 W. At the same time, the grating period of the structure is set as 510 μm. The three surfaces of the triangular prism shape are fabricated one by one. After the first surface is finished, the two disks are turned simultaneously along the axial direction with a twist angle of 120°. Then, the second surface of the triangular prism shape is prepared by the same method above. The third surface is prepared in a similar process. Finally, the periodic triangular-shaped structure is obtained.

Figure 2 shows the original transmission spectrum of the TPS-LPFG, where the resonant peak of this structure is 1368 nm, and the loss of the peak is −27 dB. The schematic diagram of the TPS-LPFG is provided in Fig. 3(a). The length of the structure is 5.6 mm, which is around one quarter the length of conventional LPFGs[8]. The lengths of the polished and unpolished

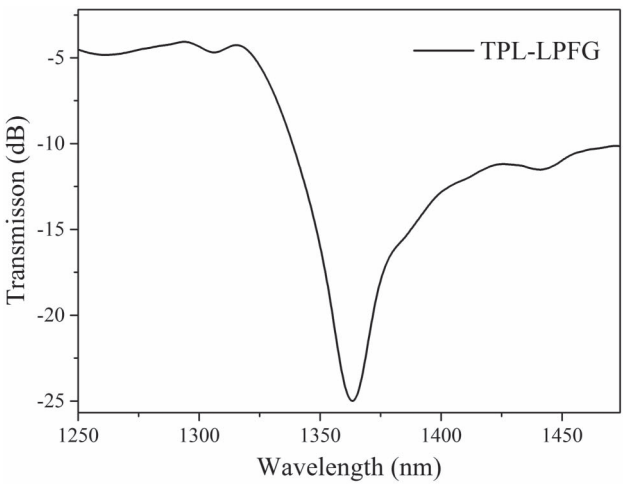

Fig. 2. Original transmission spectrum of the TPS-LPFG.

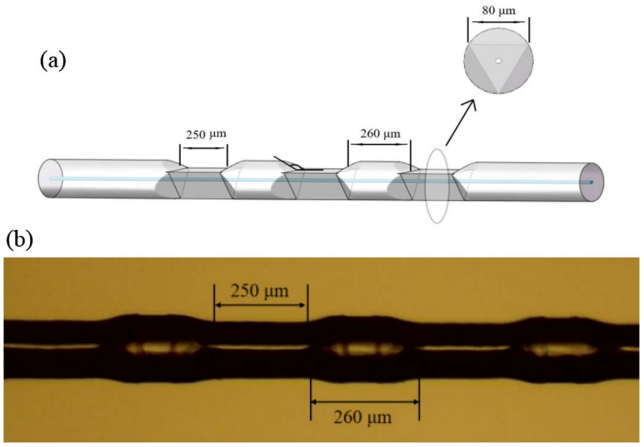

Fig. 3. Geometric characteristic of the TPS-LPFG. (a) Schematic diagram of the TPS-LPFG. (b) Side view of the TPS-LPFG.

regions are 250 μm and 260 μm, respectively. The polished depth is 35 μm, the surface of the polished area is relatively smooth, and the side view of the structure is shown in Fig. 3(b).

The mechanism of the TPS-LPFG can be attributed to the released residual stress and changed fiber geometry. These impacting aspects lead to a periodic refractive index modulation in the optical fiber[12]. The mode effective refractive index change of TPS-LPFG is calculated by

$$\delta n_{\text{eff}} = \bar{\delta} n_{\text{eff}}(z)\left\{1 + \nu \cos\left[\frac{2\pi}{\Lambda} z + \phi(z)\right]\right\}, \tag{1}$$

where $\bar{\delta} n_{\text{eff}}(z)$ is the refractive index variation in a single period of the structure, ν is the fringe visibility, Λ is the grating period, and $\phi(z)$ indicates the grating chirp.

Referring back to Fig. 2, the principle of the resonant peak generation is the light coupling between the fundamental core mode and the cladding mode. The phase-matching condition for the TPS-LPFG is demonstrated by

$$\lambda_{\text{res}} = \left[1 + \frac{(\delta n_{\text{eff}}^{\text{co}} - \delta n_{\text{eff}}^{\text{cl}}) \mathrm{d}\lambda_D / \mathrm{d}\Lambda}{(n_{\text{eff}}^{\text{co}} - n_{\text{eff}}^{\text{cl}})^2}\right](n_{\text{eff}}^{\text{co}} - n_{\text{eff}}^{\text{cl}})\Lambda, \tag{2}$$

where λ_{res} and λ_D, respectively, represent the resonant wavelength and the initial resonant wavelength, $n_{\text{eff}}^{\text{co}} - n_{\text{eff}}^{\text{cl}}$ is the effective refractive index difference between the core and cladding modes, and $\delta n_{\text{eff}}^{\text{co}} - \delta n_{\text{eff}}^{\text{cl}}$ is the average effective refractive index difference of the core and cladding modes[13]. It is clear that the sensing effects are mostly induced by the differential change of the optical fiber core and cladding modes.

For a uniform fiber to an applied torque, the twist rates are inversely proportional to the fourth power of the radius[14]. For the TPS-LPFG structure, the radii of the triangular-shaped cladding are smaller than that of the columniform-shaped fiber. When the TPS-LPFG structure is twisted, the excessive stresses are generated in the polished area. According to elasto-optic

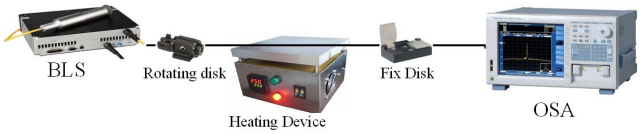

Fig. 4. Devices for torsion and temperature measurement.

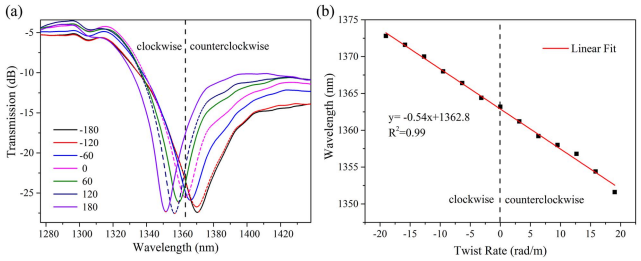

Fig. 5. Torsion characteristics of TPS-LPFG. (a) Spectrum of torsion response. (b) Measured resonant wavelength shift of different applied twist rate.

effect, the refractive index of the fiber cladding is changed by the torsional stress[15]. Hence, the difference in the effective refractive index between the core and cladding is changed. From Eq. (2), the resonant peak shifts when the optical fiber structure twists. Meanwhile, the refractive index distribution within the cross section of the TPS-LPFG is asymmetric. Hence, the linear birefringence will be induced when the light propagation in the TPS-LPFG is due to the asymmetric geometrical shape of the structure[16]. When a strong twist is applied in the structure, elliptical birefringence appears. The ratio of the semi-maximum and semi-minimum axes of the elliptical polarizations is proportional to the torsion rate[17]. The TPS-LPFG twists clockwise, and right-rotatory elliptical birefringence is generated, whereas left-rotatory elliptical birefringence results from twisting the structure counterclockwise. Thus, a torsion sensor based on

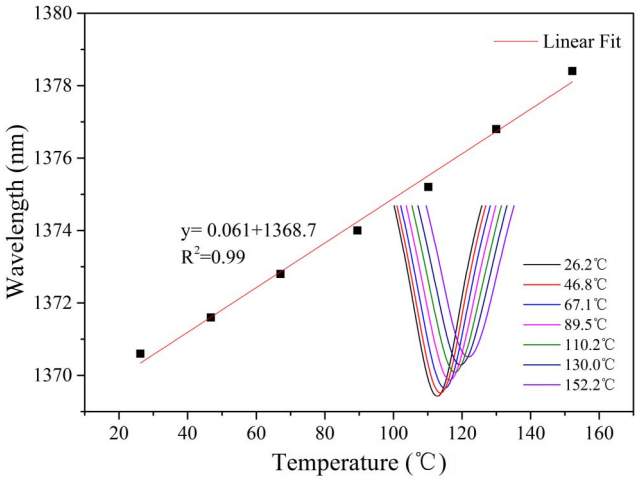

Fig. 6. Temperature characteristics of TPS-LPFG.

TPS-LPFG achieves a relatively high torsion sensitivity, and it has the ability of distinguishing the torsion direction.

3. Experiment

The schematic diagram of the experimental setup for torsion measurement is shown in Fig. 4. An SLS and an OSA are used to analyze and demodulate the wavelength spectrum. The TPS-LPFG is fixed at the middle position of two fiber disks with a 5 g weight to provide constant stress. To introduce controllable torsion, any one of the rotatory disks is rotated around the axial direction. Different torsion directions are applied by rotating the disk clockwise and counterclockwise, respectively. The torsion experiment of the structure is achieved by turning the rotating disk from −180° to 180° with a step length of 30° at room temperature.

Table 1. Comparison of the Torsion Sensitivity and Length between the TPS-LPFG and Other Sensors.

Fiber	Structure	Sensitivity [nm/(rad/m)]	Length (mm)	Reference
SMF	Corrugated LPFGs	0.18	20	[5]
SMF	LPFG written by high-frequency CO_2 laser pulses	0.03	24	[8]
SMF	LPFG based on periodical screw-type distortions	0.16	12.6	[9]
Two-mode fiber	Helical LPFGs	0.05	24	[10]
SMF	Segmented LPFG	0.14	24.5	[11]
SMF	LPFG fabricated by femtosecomd laser pulses	0.11	34.2	[18]
PCF	Helical photonic crystal fiber	0.05	50	[19]
SMF	Chirp LPFG written in twisted fiber	0.21	25	[20]
SMF	**TPS-LPFG**	**0.54**	**5.6**	**This work**

The torsion rate can be expressed by

$$\tau = \frac{\theta}{L}, \tag{3}$$

where τ is the twisting rate, θ is the torsion rate, and L is the distance between the two disks ($L = 165$ mm in the present experiment). According to Eq. (3), the torsion rate is set from -19.03 rad/m to 19.03 rad/m with a step length of 3.18 rad/m. Figure 5(a) shows the change in the transmission spectra of the TPS-LPFG. It can be seen that the resonant wavelength of the structure shows a linear red-shift when the torsion is applied clockwise and a linear blue-shift when counterclockwise torsion is applied. After conducting a linear fitting to the experimental data, the shift of the resonant peak has a linear relationship with the torsion rate, as is shown in Fig. 5(b). The torsion sensitivity of the TPS-LPFG reaches -0.54 nm/(rad/m).

In temperature measurement, the TPS-LPFG is placed on a heating device with two ends fixed by the fiber disks, as shown in Fig. 4. The temperature is controlled by the heating controller from 30°C to 150°C with a step of 20°C. Figure 6 shows that the resonant wavelength experiences a red-shift when the temperature increases, and the temperature sensitivity of the structure is 61 pm/°C. The temperature torsion crosstalk of TPS-LPFG torsion sensor is 0.11 (rad/m)/°C, which is lower than that of most conventional LPFG torsion sensors[8–10].

A comparison of the present TPS-LPFG and previous work is listed in Table 1. It can be seen that most LPFGs are about 20 mm in length. As a comparison, the TPS-LPFG is much shorter than most LPFGs in the length, and it has an enhanced torsion sensitivity. Meanwhile, the TPS-LPFG is readily fabricated at a low cost, which shows the superior features with respect to other compact LPFGs.

4. Conclusion

A novel fiber torsion sensor based on TPS-LPFG is developed in this paper. Distinguishing from the conventional fabrication method of LPFGs, the proposed fabricating method utilizes the heating effect of a CO_2 laser pulse to induce apparent deformations on the fiber. The torsion sensitivity of the sensor is -0.54 nm/(rad/m) in the preliminary experiment, which is much higher than that of conventional LPFGs, and it has a compact length. Meanwhile, this sensor can distinguish the torsion direction. The temperature sensitivity of the sensor is also provided, which is 61 pm/°C. Therefore, the proposed TPS-LPFG has great potential for torsion measurement applications, and it provides a new idea for the optical fiber torsion sensor.

Acknowledgement

This work was supported by the Joint Research Fund in Astronomy under cooperative agreement between the National Natural Science Foundation of China (NSFC) and Chinese Academy of Sciences (CAS) (Nos. U1831115, U1631239, and U1931206), the Dean Project of Guangxi Key Laboratory of Wireless Broadband Communication and Signal Processing (No. GXKL06190106), and the Key Projects of Natural Science Foundation of Heilongjiang Province (No. ZD2019H003).

References

1. C. T. Sun, R. Wang, and X. R. Jin, "A new phase-shifted long-period fiber grating for simultaneous measurement of torsion and temperature," Chin. Opt. Lett. **18**, 021203 (2020).
2. Y. P. Wang, J. P. Chen, and Y. J. Rao, "Torsion characteristics of long-period fiber gratings induced by high-frequency CO_2 laser pulses," J. Opt. Soc. Am. B **22**, 1167 (2005).
3. Z. H. Hang, C. T. Sun, and X. R. Jin, "A polarization-independent torsion sensor based on the near-helical long period fiber grating," Chin. Opt. Lett. **16**, 100601 (2018).
4. X. W. Shu, L. Zhang, and I. Bennion, "Sensitivity characteristics of long-period fiber gratings," J. Lightwave Technol. **20**, 255 (2002).
5. C. Y. Lin, L. A. Wang, and G. W. Chern, "Corrugated long-period fiber gratings as strain, torsion, and bending sensors," J. Lightwave Technol. **19**, 1159 (2001).
6. D. A. Gonzalez, C. Jauregui, A. Quintela, F. J. Madruga, P. Marquez, and J. M. Lopez-Higuera, "Torsion-induced effects on UV long-period fiber gratings," Proc. SPIE **5502**, 192 (2004).
7. Y. J. Rao, Y. P. Wang, Z. L. Ran, and T. Zhu, "Novel fiber-optic sensors based on long-period fiber gratings written by high-frequency CO_2 laser pulses," J. Lightwave Technol. **21**, 1320 (2003).
8. Y. P. Wang, "Review of long period fiber gratings written by CO_2 laser," J. Appl. Phys. **108**, 081101 (2010).
9. M. Deng, J. S. Xu, Z. Zhang, Z. Y. Bai, S. Liu, Y. Wang, Y. Zhang, C. R. Liao, W. Jin, and G. D. Peng, "Long period fiber grating based on periodically screw-type distortions for torsion sensing," Opt. Express **25**, 14308 (2017).
10. L. Zhang, Y. Q. Liu, Y. H. Zhao, and T. Y. Wang, "High sensitivity twist sensor based on helical long-period grating written in two-mode fiber," IEEE Photon. Technol. Lett. **28**, 1629 (2016).
11. C. T. Sun, T. Geng, J. He, A. Zhou, W. L. Yang, X. R. Jin, X. D. Chen, Y. Zhou, Q. H. Hu, and L. B. Yuan, "High sensitive directional torsion sensor based on a segmented long-period fiber grating," IEEE Photon. Technol. Lett. **29**, 2179 (2017).
12. L. A. Wang, C. Y. Lin, and G. W. Chern, "A torsion sensor made of a corrugated long period fibre grating," Meas. Sci. Technol. **12**, 793 (2001).
13. L. L. Xian, P. Wang, and H. P. Li, "Power-interrogated and simultaneous measurement of temperature and torsion using paired helical long-period fiber gratings with opposite helicities," Opt. Express **22**, 20260 (2014).
14. L. L. Shi, T. Zhu, Y. E. Fan, K. S. Chiang, and Y. J. Rao, "Torsion sensing with a fiber ring laser incorporating a pair of rotary long-period fiber gratings," Opt. Commun. **284**, 5299 (2011).
15. C. Y. Lin and L. A. Wang, "A wavelength and loss tunable band rejection filter based on corrugated long-period fiber grating," IEEE Photon. Technol. Lett. **13**, 332 (2001).
16. R. U. lrich and A. Simon, "Polarization optics of twisted single-mode fibers," Appl. Opt. **18**, 2241 (1979).
17. B. L. Bachim and T. K. Gaylord, "Polarization-dependent loss and birefringence in long-period fiber gratings," Appl. Opt. **42**, 6816 (2003).
18. X. R. Dong, Z. Xie, Y. X. Song, K. Yin, Z. Luo, J. A. Duan, and C. Wang, "Highly sensitive torsion sensor based on long period fiber grating fabricated by femtosecond laser pulses," Opt. Laser Technol. **97**, 248 (2017).
19. X. M. Xi, G. K. L. Wong, T. Weiss, and P. S. J. Russell, "Measuring mechanical strain and twist using helical photonic crystal fiber," Opt. Lett. **38**, 5401 (2013).
20. L. Zhang, Y. Q. Liu, X. B. Cao, and T. Y. Wang, "High sensitivity chiral long-period grating sensors written in the twisted fiber," IEEE Sens. J. **16**, 4253 (2016).